proceedings

Abstract

S/C Composites with Different Carbon Matrices as Cathode Materials for Metal-Sulfur Batteries †

Svetlana Novikova [1,*], Daria Voropaeva [1], Sergey Li [2,3], Andrey Yaroslavtsev [1]

[1] Kurnakov Institute of General and Inorganic chemistry of Russian Academy of Sciences; voropaeva-dd@yandex.ru (D.V.); yaroslav@igic.ras.ru (A.Y.)
[2] Frumkin Institute of Physical Chemistry and Electrochemistry of the RAS; li.sergey.99@mail.ru
[3] Moscow Power Engineering Institute; National Research University
* Correspondence: svetlana_novi@mail.ru
† Presented at the 1st International Electronic Conference on Processes: Processes System Innovation, 17–31 May 2022; Available online: https://ecp2022.sciforum.net.

Abstract: This work is devoted to comparative study of the electrochemical properties of S/C composites with different carbon matrices such as carbon nanotubes, mesoporous carbon and N-doped carbon nanoflakes as cathode materials for lithium- and sodium-sulfur batteries. The best among the investigated samples was composite based on sulfur and mesoporous carbon (S/MC) due to the partial encapsulation of the sulfur into the pore of the mesoporous carbon. First cycle discharge capacity of S/MC in Li-S and Na-S battery cells was 1247 and 323 mAh*g-1, correspondingly. Discharge capacity of S/MC in Li-S and Na-S battery after 10 cycles was 270 and 235 mAh*g-1, correspondingly.

Keywords: lithium-sulfur batteries; sodium-sulfur batteries; cathode material; sulfur; carbon

Citation: Lastname, F.; Lastname, F.; Lastname, F. Title. *Proceedings* **2022**, *69*, x. https://doi.org/10.3390/xxxxx

Academic Editor: Firstname Lastname

Published: date

Publisher's Note: MDPI stays neutral with regard to jurisdictional claims in published maps and institutional affiliations.

1. Introduction

Metal-sulfur battery technology promises much higher energy storage capacity compared to common Li-ion commercial batteries (theoretical capacity of lithium, sodium and sulfur amount to 3860, 1165 and 1672 mAh/g). Sulfur undergoes through a conversion reaction and forms lithium or sodium polysulfides [1-3], allowing larger accommodation of two ions and electrons per sulfur atom [2, 4]. At the same time, sulfur is a non-toxic abundant and low-cost element. This explains the interest in lithium-sulfur batteries and sodium-sulfur batteries capable of operating at room temperature (RT-Na/S batteries). Unfortunately, few issues are still hindering their commercialization. Among them low electrical conductivity of sulfur, significant change in the volume of the cathode during the discharge/charge process, migration of soluble polysulfides of alkali metal between electrodes should be mentioned. [3,5]. In this regard, in recent years, much attention has been paid to the development of materials for metal-sulfur batteries. Among the above problems, the mitigating the shuttle effect is the most important. To overcome this problem such approached as composite cathode formation, covalent sulfur bonding, the use of electrocatalyst-containing cathodes, inserting an interlayer or selective separators are used [5, 6].

This work is devoted to comparative study of the electrochemical properties of S/C composites with different carbon matrices such as carbon nanotubes (CNT), mesoporous carbon (MC) and N-doped carbon nanoflakes (N-CNF) as cathode materials for lithium- and sodium-sulfur batteries.

2. Methods

Carbon nanotubes (Taunit-MD) and mesoporous carbon was industrially obtained (NanoTechCenter LTD, Russia). Synthesis of N-doped carbon nanoflakes was described elsewhere [7]. Carbon materials were purified from remains of the catalyst used in the synthesis according to manufacturer's procedures: materials were suspended in 30% (by weight) HNO_3 in 1:8 weight ratio and the suspension was kept for 1 h at 90 °C with continuous stirring. After that, they were washed with a large amount of water to neutral pH and dried in air for 24 h at 90 °C.

Sulfur loaded composite materials with carbon were prepared by the conventional melt diffusion method. The prepared MC, CNT and N-CNF were ground with elemental sulfur in a mass ratio of 1:1. It was mixed well and placed in a glove box filled with argon for 10 min. The reaction was carried out in a Teflon-lined reactor at 155 °C for 20 h. Finally, the samples S/MC, S/CNT and S/N-CNF were obtained.

X-ray diffraction (XRD) analysis was performed with the use of a Rigaku D/MAX 2200 diffractometer (CuKα). The XRD patterns were analyzed using the Rigaku Application Data Processing software. Microstructure analysis of the samples was performed using a scanning electron microscope (SEM) TESCAN AMBER GMH. The specific surface area was studied by the BET method using a Sorbtometr-M analyzer (LLC Katakon). The samples were degassed at 200 °C for 1 h prior to the measurement. Raman spectra were collected using DXRxi Raman Imaging Microscope (Thermo Fisher Scientific). A 532 nm laser with power of 0.2–0.6 mW was used.

Electrochemical testing of the S/C composites was carried out in the sealed three electrode cells with lithium (or sodium) as counter and reference electrodes. The working electrodes were manufactured by the standard casting technology. The active paste was prepared by mixing the S/C composite with carbon black (Ketjen Black) and polyvinylidene fluoride (Kynar) dissolved in N-methyl-2-pyrrolidone (NMP) with the mass ratio of 85/10/5. The slurry was coated on stainless steel substrate and then dried in a vacuum oven at 50 °C until NMP evaporation. The electrodes were pressed under a 1000 kg/cm^2 pressure and then vacuum-dried at 50 °C for 16 h. The electrochemical cells were assembled in a high-purity argon-filled glove box with the content of water and oxygen ≤1 ppm (Spectroscopic Systems) using non-woven polypropylene separator. 1 M Li_2NH in a dioxolane/dimethoxyethane (1:1 by volume) or 1M $NaClO_4$ in a triglim was used as the electrolyte. The water content in the electrolyte measured by Fischer titration (917 Coulometer, Metrohm) did not exceed 30 ppm. The cyclic voltammetry (CV) results were obtained with a P-20X potentiostat (Elins) at a scan rate of 0.1mV/s. The values of capacity were calculated on the content of sulfur.

3. Results and Discussion

The specific surface area of the carbon materials used in this work for S/C composite formation is equal to 3200, 270 and 1028 m^2*g^{-1} for MC, CNT and N-CNF, correspondingly. In the Raman spectra of MC and N-CNF an intensive band with a maximum at ~1590 cm^{-1} can be assigned to the G-band of crystalline graphite (sp^2-hybridized carbon) and a band at ~1350 cm^{-1} to the D-band of disordered graphite. Along with them, two wide bands can be distinguished around 1200 and 1500 cm^{-1}, corresponding to the carbon fragments with different structure. For example, the band at 1500 cm^{-1} can be assigned to vibrations of sp^3-hybridized carbon [8]. The contribution of these additional bands amounts to 40% for MC and 47% for N-CNF. This indicates that the carbon coating is represented mainly by sp^2-hybridized carbon. The ratio of the integral intensities of D- and G-bands can be used to estimate the degree of defectiveness of carbon materials (ID/IG). The ID/IG are lower for MC (2,7 for MC and 3,7 for N-CNF).

The XRD patterns of MC, CNT and N-CNF are presented by poorly resolved diffraction peak at 2Θ of ~24-26° that can be assigned to the [002] crystallographic plane of graphene. This reflection also can be corresponding to CNTs [7]. The peak position shifts to the smaller angles in the series CNT, MC, N-CNF and the interplanar spacing

correspondingly increases. The XRD patterns of the S/CNT, S/N-CNF samples are combinations of XRD patterns of sulfur and the corresponding carbon material of a noticeably lower intensity. The XRD pattern of S/MC contain no peaks of S. The decrease of intensity or disappearance of peaks of sulfur can be attributed to the reduced size of the sulfur after sulfur loading process and the successful encapsulation of sulfur in the pores of MC for S/MC.

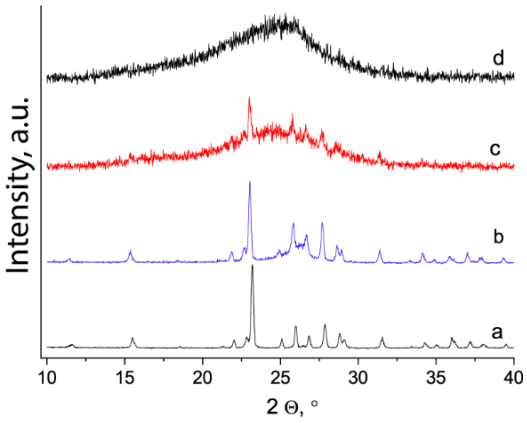

Figure 1. Fragments of XRD patterns of the sulfur (a), S/CNT (b), S/N-CNF (c) and S/MC (d) in the region of 2Θ = 10-40°.

The typical SEM images of the samples obtained are presented on Fig. 2. In the S/CNT composite (Fig. 2 a,b) sulfur is distributed rather uniformly over the carbon material, that forms a conductive support. In the S/N-CNF and S/MC samples one can see both homogeneous regions and agglomerates of sulfur (Fig. 2 c,d).

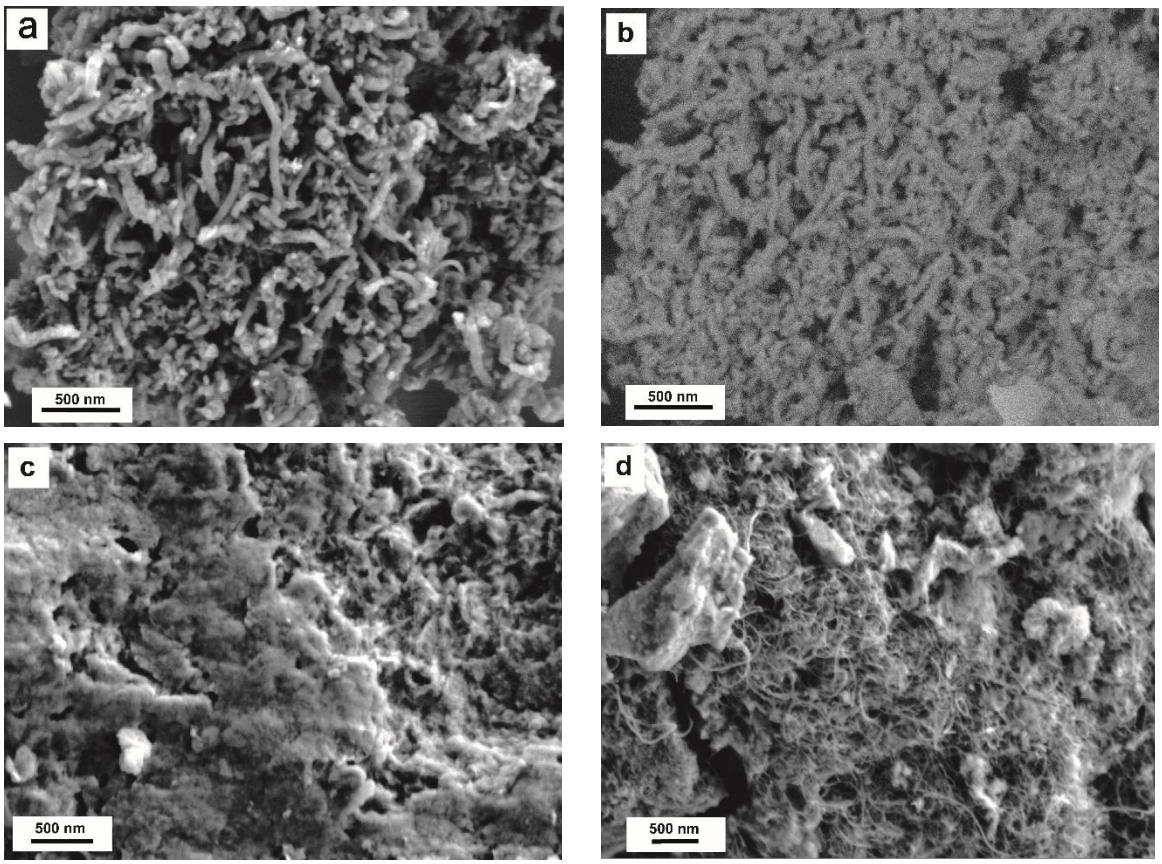

Figure 2. SEM images in the secondary (a, c, d) and backscattered (b) electron modes of the S/CNT (a,b), S/N-CNF (c) and S/MC (d) composites.

CV measurements for Li-S cells were performed within a potential range of 1.4–3 V. One main anodic peak and two cathodic peaks are caused by electrochemical conversion of element sulfur and Li-polysulfides. The typical characteristic peaks of S/MC is displayed in Fig. 3 (a). CV curves of S/CNT show similar shapes, reflecting that the same reaction process and reversible transformations occur. The CV curves of the S/N-CNF are differ compared with S/MC (Fig. 3 (a)). The reduction and oxidation peaks of S/N-CNF occur at lower and higher peak voltages, respectively, than those of S/MC. The peak currents are lower indicating worse electrochemical reaction kinetics of Li-S battery. Discharge capacities of S/MC and S/CNT amount to 1247 and 585 mAh*g^{-1} correspondingly. However, the discharge capacity values rapidly decreased during cycling. The discharge capacity was 270 and 237 on the 10th cycle for S/MC and S/CNT, respectively. The decrease of capacities is most likely resulting from the dissolution of polysulfides and the detachment of active materials. S/MC was the best among investigated samples due to the partial encapsulation of the sulfur into the pore of the mesoporous carbon. Cyclic performance of the S/MC represented on Fig 3 (b).

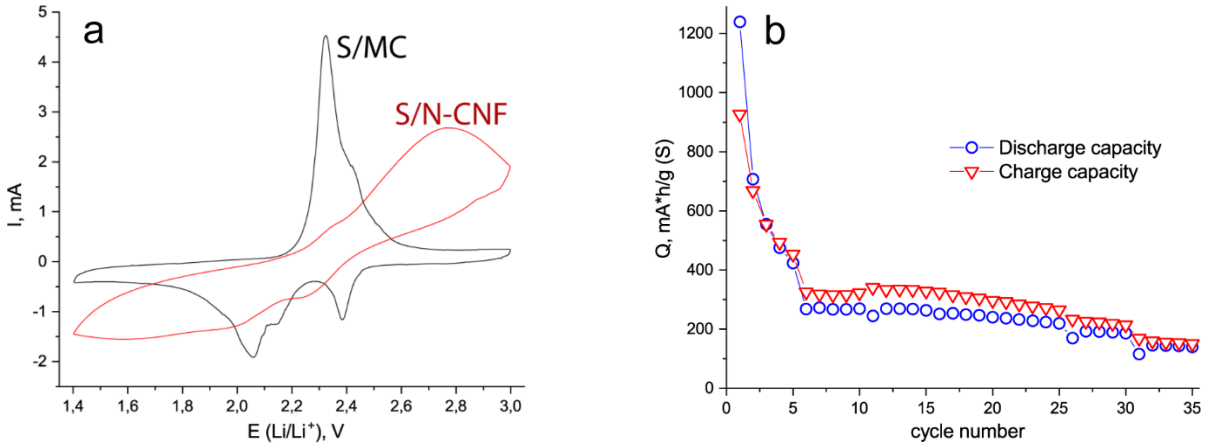

Figure 3. CV curves of the S/MC and S/N-CNF (a) and cyclic performance of the S/MC (b).

The sample S/MC was tested in a sodium-sulfur cell. CV measurements for Na-S cells were performed within a potential range of 1–3 V. CV curves are typical for RT-Na-S batteries and show cathodic waves at ~2.2 and ~1.6 V [3]. There are differences in the anodic waves between the Li-S and Na-S cells. The Na-S cells show two clean-cut oxidation waves at ~1.9 and ~2.4 V. Discharge capacity for S/MC was 323 and 235 mAh*g^{-1} at 1 and 10 cycle, correspondingly.

4. Conclusions

S/C composites with different carbon matrices such as carbon nanotubes, mesoporous carbon and N-doped carbon nanoflakes were prepared by the conventional melt diffusion method and tested as cathodes for lithium- and sodium-sulfur batteries. The best among the investigated samples was composite based on sulfur and mesoporous carbon (S/MC) due to the partial encapsulation of the sulfur into the pore of the mesoporous carbon. First cycle discharge capacity of S/MC in Li-S and Na-S battery cells was 1247 and 323 mAh*g^{-1}, correspondingly. Discharge capacity of S/MC in Li-S and Na-S battery after 10 cycles was 270 and 235 mAh*g^{-1}, correspondingly.

Conflict of Interest: The authors declare no competing financial interest.

Acknowledgements: This work was supported by the Ministry of Science and Higher Education of the Russian Federation as part of the State Assignment of the Kurnakov

Institute of General and Inorganic Chemistry of the Russian Academy of Sciences. This research was performed using the equipment of the JRC PMR IGIC RAS.

References

1. A.N. Mistry, P.P. Mukherjee, Journal of Physical Chemistry C, 122 (2018) 23845-23851 doi: 10.1021/acs.jpcc.8b06077.
2. A. Manthiram, X.W. Yu, Small, 11 (2015) 2108-2114 doi: 10.1002/smll.201403257.
3. X.W. Yu, A. Manthiram, Adv. Funct. Mater., 30 (2020) doi: 10.1002/adfm.202004084.
4. W.M. Kang, N.P. Deng, J.G. Ju, Q.X. Li, D.Y. Wu, X.M. Ma, L. Li, M. Naebe, B.W. Cheng, Nanoscale, 8 (2016) 16541-16588 doi: 10.1039/c6nr04923k.
5. A. Manthiram, Y.Z. Fu, S.H. Chung, C.X. Zu, Y.S. Su, Chem. Rev., 114 (2014) 11751-11787 doi: 10.1021/cr500062v.
6. L. Wang, T. Wang, L. Peng, Y. Wang, M. Zhang, J. Zhou, M. Chen, J. Cao, H. Fei, X. Duan, J. Zhu, X. Duan, Natl. Sci. Rev., (2021) doi: 10.1093/nsr/nwab050.
7. I.A. Stenina, R.R. Shaydullin, A.V. Desyatov, T.L. Kulova, A.B. Yaroslavtsev, Electro-chim. Acta, 364 (2020) doi: 10.1016/j.electacta.2020.137330.
8. J.D. Wilcox, M.M. Doeff, M. Marcinek, R. Kostecki, J. Electrochem. Soc., 154 (2007) A389-A395 doi: 10.1149/1.2667591.